

SUCCESSFUL COMBINATION OF FERROMAGNETISM AND PHOTOLUMINESCENCE PROPERTIES IN LEAD-FREE FERROELECTRIC $\text{Bi}_{0.5}\text{Na}_{0.5}\text{TiO}_3$ MATERIALS

Nguyen The Hung^{1,2} and Dang Duc Dung¹

¹*Department of General Physics, School of Engineering Physics,
Hanoi University of Science and Technology*

²*Faculty of Basic, Fundamental Sciences, Vietnam Maritime University*

Abstract. Lead-free ferroelectric $\text{Bi}_{0.5}\text{Na}_{0.5}\text{TiO}_3$ materials integrated ferromagnetism and photoluminescence at room temperature. Fe and Sm cations were used as the magnetic and photoluminescence sources for the co-modified host $\text{Bi}_{0.5}\text{Na}_{0.5}\text{TiO}_3$ materials. The (Fe, Sm)-modified $\text{Bi}_{0.5}\text{Na}_{0.5}\text{TiO}_3$ materials were fabricated by using the sol-gel method. The structure of the samples was studied through X-ray diffraction and Raman scattering, which indicated that a single perovskite structure was successfully fabricated. The samples exhibited strong photoluminescence in the visible light range, and complex ferromagnetic properties were obtained. We expect our work to open a new direction in the development of advanced function materials for smart electronic device applications.

Keywords: $\text{Bi}_{0.5}\text{Na}_{0.5}\text{TiO}_3$, lead-free ferroelectric, ferromagnetic, photoluminescent, sol-gel.

1. Introduction

The development of green materials for smart electronic applications is the next research trend. Ferroelectric Pb-based materials are widely used in electronic devices, because they exhibit excellent piezoelectric, ferroelectric, and dielectric properties [1, 2]. However, the toxicity of Pb with high chemical composition (approximately 60% wt.) hindered the materials' further application to electronic devices because of their possible threat to human health and concerns regarding environmental pollution [2, 3]. Therefore, the use of green ferroelectric materials as a replacement of lead-based ferroelectric materials in electronic devices needs to be investigated.

Among lead-free ferroelectric materials, $\text{Bi}_{0.5}\text{Na}_{0.5}\text{TiO}_3$ -based materials were recently reported to exhibit physical properties that are superior to those of $\text{Pb}(\text{Zr},\text{Ti})\text{O}_3$

Received August 28, 2019. Revised October 22, 2019. Accepted October 29, 2019.

Contact Dang Duc Dung, e-mail address: dung.dangduc@hust.edu.vn

materials [4]. $\text{Bi}_{0.5}\text{Na}_{0.5}\text{TiO}_3$ materials were first fabricated in 1960 [5]. They have a large remnant polarization ($P_r \approx 38 \mu\text{C}/\text{cm}^2$) and a high Curie temperature ($T_C \approx 320 \text{ }^\circ\text{C}$) but have low piezoelectric constants, because the high coercive field ($E_C \approx 7.3 \text{ kV}/\text{mm}$) of the samples result in poling difficulties under an external electric field [4, 5]. $\text{Bi}_{0.5}\text{Na}_{0.5}\text{TiO}_3$ materials have a piezoelectric coefficient (d_{33}) of approximately 74-94.8 pC/N and a dielectric constant (ϵ_r) of 425 at room temperature [6-8]. Thanh *et al.* reported that $\text{Bi}_{0.5}\text{Na}_{0.5}\text{TiO}_3$ materials have an optical band gap in the range of 3.00 eV to 3.14 eV, which depends on the fabrication method [9]. In addition, the photoluminescence properties of pure $\text{Bi}_{0.5}\text{Na}_{0.5}\text{TiO}_3$ materials are mostly related with the surface effect, in which the unsaturation bonding of elements at the surface causes the local defect, thereby resulting in the transition of photon absorption [10]. Typical $\text{Bi}_{0.5}\text{Na}_{0.5}\text{TiO}_3$ materials exhibit a major diamagnetic behavior resulting from an empty $3d^0$ cell orbital [11]. The weak-ferromagnetism in $\text{Bi}_{0.5}\text{Na}_{0.5}\text{TiO}_3$ materials are related with self-defects, such as Na and Ti-vacancies [11-13]. The experimental observation of ferromagnetism in non-stoichiometry $\text{Bi}_{0.5}\text{Na}_{0.5}\text{TiO}_3$ materials is consistent with the theoretical investigation where magnetism was mostly induced from Na or Ti-vacancies, whereas Bi or O vacancies were less affected [14]. However, the main problem is that the magnetization of self-defect induced magnetism was too small, that is, normally less than 1 memu/g [10-13]. The low magnetization and photoluminescence of $\text{Bi}_{0.5}\text{Na}_{0.5}\text{TiO}_3$ materials limit their application to smart electronic devices, which require many functions with excellent properties.

In fact, the development of magnetic and photoluminescence properties for $\text{Bi}_{0.5}\text{Na}_{0.5}\text{TiO}_3$ materials have been reported separately. The magnetic properties of $\text{Bi}_{0.5}\text{Na}_{0.5}\text{TiO}_3$ materials have been developed by doping of transition metals, such Fe, Co, and Mn [12, 15, 16]. In addition, we recently reported that the magnetic properties of $\text{Bi}_{0.5}\text{Na}_{0.5}\text{TiO}_3$ materials are strongly enhanced via the co-modification of the A- and B-sites in the perovskite structure through alkali-earth and transition metals, such $\text{SrFeO}_{3-\delta}$, $\text{MgFeO}_{3-\delta}$, and $\text{MgMnO}_{3-\delta}$ [10, 17, 18]. Similarly, strong photoluminescence properties were obtained for $\text{Bi}_{0.5}\text{Na}_{0.5}\text{TiO}_3$ materials using rare earth materials as impurities, such as Nd, Er, Eu, Sm, and Pr [19-23]. To date, the combination of ferromagnetism and photoluminescence in lead-free ferroelectric $\text{Bi}_{0.5}\text{Na}_{0.5}\text{TiO}_3$ materials has not been intensively investigated.

In this work, ferromagnetism and photoluminescence were integrated in lead-free ferroelectric materials by co-dopants using transition and rare earth metals. For testing, 5 mol.% of Sm and Fe co-doped $\text{Bi}_{0.5}\text{Na}_{0.5}\text{TiO}_3$ materials were successful fabricated by sol-gel method. The samples exhibited strong ferromagnetism and photoluminescence at room temperature.

2. Content

2.1. Experiments

$(\text{Bi}_{0.5}\text{Na}_{0.5})_{0.95}\text{Sm}_{0.05}\text{Na}_{0.5}\text{Ti}_{0.95}\text{Fe}_{0.05}\text{O}_3$ (BNSTFO) materials were fabricated by sol-gel method. The raw materials used were bismuth (III) nitrate pentahydrate ($\text{Bi}(\text{NO}_3)_3 \cdot 5\text{H}_2\text{O}$), sodium nitrate (NaNO_3), iron (III) nitrate ($\text{Fe}(\text{NO}_3)_3 \cdot 9\text{H}_2\text{O}$),

samarium nitrate ($\text{Sm}(\text{NO}_3)_3 \cdot 6\text{H}_2\text{O}$), and tetra isopropoxy titanium (IV) ($\text{C}_{12}\text{H}_{28}\text{O}_4\text{Ti}$). Acid acetic (CH_3COOH) and acetylacetonone ($\text{CH}_3\text{COCH}_2\text{COCH}_3$) were used as the ligand. $\text{Bi}(\text{NO}_3)_3 \cdot 5\text{H}_2\text{O}$ was weighed and dissolved in acid acetic by magnet stirring until transparent. Thus, NaNO_3 , $\text{Sm}(\text{NO}_3)_3 \cdot 6\text{H}_2\text{O}$, and $\text{Fe}(\text{NO}_3)_3 \cdot 9\text{H}_2\text{O}$ were weighed and then added under magnetic stirring. Acetylacetonone was added to the solution before the dropwise addition of tetra isopropoxy titanium (IV) to prevent the formation of hydroxyls of cation titanium in the solution. The solution was kept under magnet stirring for approximately 3 h until a homogenous sol was obtained. The sols were heated at 100 °C to prepare the dry gel. The gels were annealed in air at 800 °C for 3 h. Then, the as-prepared samples were naturally cooled to room temperature. Given that sodium is a light element and easily evaporates during the gelling and sintering processes, excessive sodium was added to approximately 50 mol.% from sodium nitrate sources [9-12]. The crystal structure of the samples was characterized through X-ray diffraction (XRD). The phonon vibrational modes of the samples were measured through Raman scattering. The optical properties of the samples were characterized by ultraviolet–visible spectroscopy (UV-Vis) and photoluminescence (PL). The magnetic properties of the samples were measured using a vibrating sample magnetometer (VSM). All measurements were obtained at room temperature.

2.2. Results and discussion

Figure 1 shows the X-ray diffraction spectra of the BNSTFO samples in the 2 θ range from 20° to 70°. The peak position and intensity of the pure $\text{Bi}_{0.5}\text{Na}_{0.5}\text{TiO}_3$ materials were indexed for the rhombohedral structure. The results also showed multi-diffraction peaks, thereby suggesting that the samples have a single perovskite structure with polycrystalline. The impurity phases were not obtained based on the limitation of XRD method, indicating that the single-phase BNSTFO samples were fabricated by sol-gel method. The results are consistent with the modified- $\text{Bi}_{0.5}\text{Na}_{0.5}\text{TiO}_3$ materials obtained by sol-gel method [17, 18]. Based on Shannon's report, the radii of Sm^{3+} , Bi^{3+} , and Na^+ cations are 1.24 Å (in coordination number 12), 1.17 Å (in coordination number 8), and 1.39 Å (in coordination number 12), respectively, whereas those of $\text{Fe}^{3+/2+}$ and Ti^{4+} cations in coordination number 6 are 0.645 Å/0.780 Å and 0.605 Å, respectively [24]. Therefore, we suggested that Sm^{3+} cations trended to random incorporation with A-site (Bi^{3+} - and/or Na^+ -site) while $\text{Fe}^{2+/3+}$ cations were possible substituted for B-site (Ti^{4+} -site). In other word, Fe and Sm cations were successful incorporated into the crystal of the host $\text{Bi}_{0.5}\text{Na}_{0.5}\text{TiO}_3$ materials.

Figure 2 shows the Raman scattering of the BNSTFO samples in the frequency range of 250 cm^{-1} to 1250 cm^{-1} . The broad bands in Raman scattering were obtained where the Raman peaks were not obvious and overlapped. The overlapping Raman scattering peaks and regions are related with the random distribution of Bi^{3+} and Na^+ cations at the A-site in the perovskite structure [25]. The theoretical calculation for the vibration modes in pure $\text{Bi}_{0.5}\text{Na}_{0.5}\text{TiO}_3$ materials indicates that the Raman scattering modes from 109-134 cm^{-1} were related to the displacements of Bi ions, and the high frequency modes from 155-187 cm^{-1} were assigned to the Na–O vibrations [25]. The TiO_6 vibration was related to the frequency range of 246–401 cm^{-1} , whereas the

vibration of the oxygen atoms was observed from 413 cm^{-1} to 826 cm^{-1} [25]. Zhu *et al.* reported that the TiO_6 vibration was active from 450 cm^{-1} to 700 cm^{-1} , whereas the Ti-O vibration was observed from 150 cm^{-1} to 450 cm^{-1} [26]. The TO_3 mode at approximately 541 cm^{-1} may be due to the symmetric O-Ti-O stretching vibration of the octahedral $[\text{TiO}_6]$ cluster, whereas the LO_3 modes found at 813 cm^{-1} are due to the presence of the sites within the rhombohedral lattice containing distorted octahedral $[\text{TiO}_6]$ clusters [27, 28].

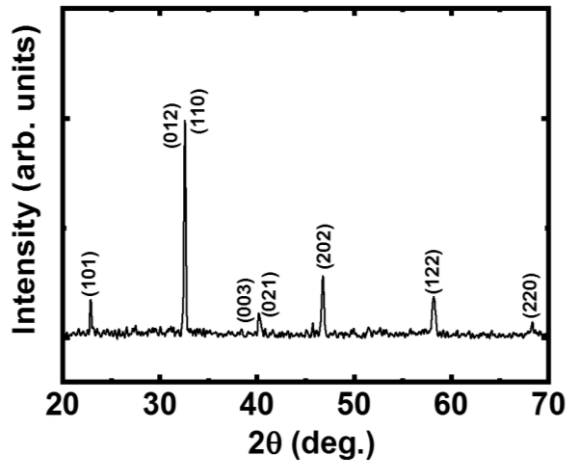


Figure 1. X-ray diffraction pattern of BSNTFO samples

Barick *et al.* suggested that high frequency bands, such as the 486 , 526 , and 583 cm^{-1} band of perovskite titanate materials, are dominated by a vibration that involves oxygen displacements [29]. However, unlike theoretical investigations, a high frequency was obtained in our experimental. Thus, we suggest that the high frequency was related with oxygen vacancies. Therefore, on the basis of the XRD and Raman scattering and the structural and vibration modes of the BNSTFO samples, we further confirmed that our BNSTFO samples have a single-phase with a polycrystal structure.

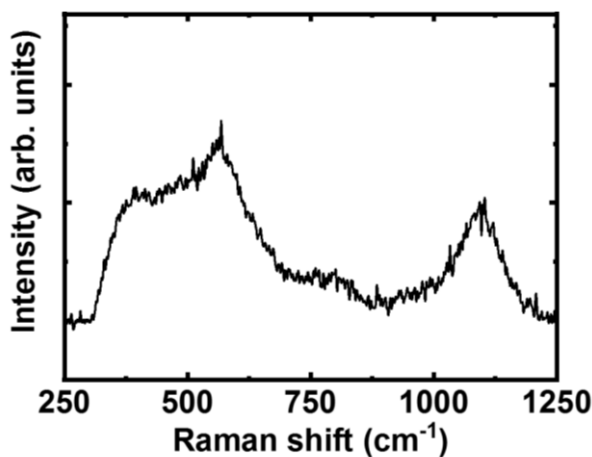


Figure 2. The Raman scattering of BSNTFO samples

Figure 3 (a) shows the UV-Vis spectra of the BNSTFO sample at room temperature. The samples did not exhibit a single transition where the multi-edge transition was obtained. Recently, the optical properties of $\text{Bi}_{0.5}\text{Na}_{0.5}\text{TiO}_3$ materials exhibited a single absorbance band with a slight tail [9-12]. The slight tail in the absorbance of pure $\text{Bi}_{0.5}\text{Na}_{0.5}\text{TiO}_3$ materials was related to the surface effect and/or the self-defect [9-12].

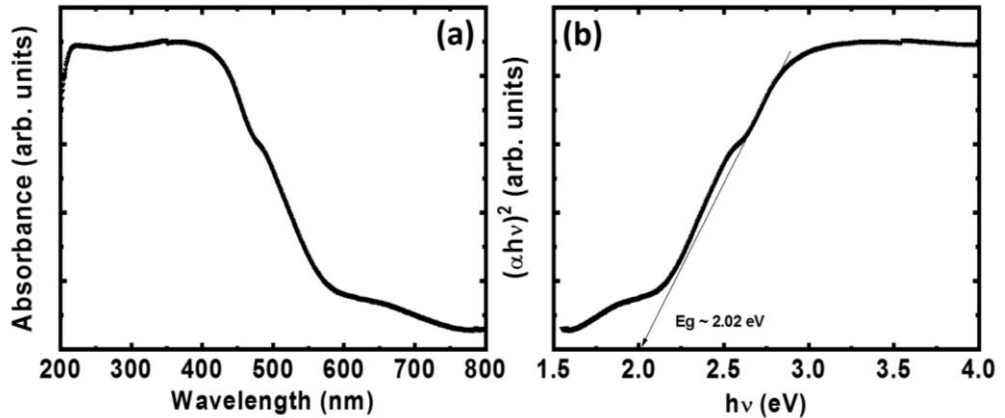


Figure 3. (a) The UV-Vis of BNSTFO samples, and (b) the plotted of $(\alpha h\nu)^2$ as function of absorption photon energy ($h\nu$)

The calculation of the electronic band structure by first principles analysis indicates that the $\text{Bi}_{0.5}\text{Na}_{0.5}\text{TiO}_3$ materials directly transitioned from the interband transition, from the O 2*p* valence bands to the Ti 3*d* and/or Bi 6*p* conduction bands in the low-energy region, where the valence band was built from the hybridization between O 2*p* and Ti 3*d*, and the Bi 6*p* states and the conduction band were constructed from the Ti 3*d*, Bi 6*p*, and Na 2*s* states and the hybridized O 2*p* states [30]. In addition, the *ab initio* calculations of the electronic band structure of the $\text{Bi}_{0.5}\text{Na}_{0.5}\text{TiO}_3$ materials also predicted the appearance of natural vacancies, such as Na, Ti, and O, thereby resulting in new induced states in the near conduction band [13]. Ju *et al.* also predicted that the Na vacancies at the grain surfaces are tuned to the electronic band structure of the $\text{Bi}_{0.5}\text{Na}_{0.5}\text{TiO}_3$ materials [13]. Therefore, the E_g values of the BNSTFO sample materials were estimated from the $(\alpha h\nu)^2$ plot with absorption photon energy ($h\nu$), where α is the coefficient, h is the Plank constant, and ν is the frequency of the photon energy, as shown in Figure 3 (b). Thus, the E_g values were calculated by extrapolating a straight line from the proportion of the curve or tail. The E_g values of the materials were estimated to be 2.02 eV, which is smaller than that of $\text{Bi}_{0.5}\text{Na}_{0.5}\text{TiO}_3$ materials. The reduction of the optical band gap values of the $\text{Bi}_{0.5}\text{Na}_{0.5}\text{TiO}_3$ materials via the co-doped Fe and Sm was possibly caused by the appearance of a new local state in the electronic band structure. Therefore, the modification of the optical band gap of the $\text{Bi}_{0.5}\text{Na}_{0.5}\text{TiO}_3$ materials is a solid evidence of the incorporation of Fe and Sm cations into the host crystal.

Figure 4 shows the magnetic hysteresis loop of the BNSTFO samples at room temperature. The result samples exhibit a typical ferromagnetism behavior. The coercive field and the remnant magnetization were estimated to be approximately 112 Oe and 1.2 memu/g, respectively, which are a solid evidence of ferromagnetism

ordering in BNSTFO samples. The saturation magnetization of the samples was approximately 19.5 emu/g, thereby reflecting the great enhancement of that of pure $\text{Bi}_{0.5}\text{Na}_{0.5}\text{TiO}_3$ materials.

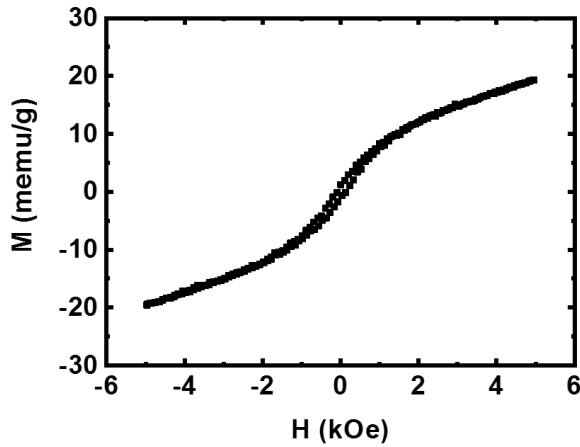


Figure 4. The magnetization as function of applied strength external magnetic field at room temperature of BSNTFO samples

The saturation magnetization of the BNSTFO samples was also approximately twice that of Fe-doped $\text{Bi}_{0.5}\text{Na}_{0.5}\text{TiO}_3$ materials at the same concentration of 5 mol.% [16]. However, the magnetization of the samples was not saturated with the increasing application of the external magnetic field. The room temperature ferromagnetism of the BNSTFO materials possibly resulted from the interaction of Fe cations through the oxygen vacancies (\square), such as the $\text{Fe}^{3+}-\square-\text{Fe}^{3+}$ pairs. The oxygen vacancies were created due to the unbalanced valence state of Fe^{3+} and Ti^{4+} , when the Fe^{3+} cations were substituted for the Ti^{4+} cations in the octahedral site. The unsaturation of the magnetic moment of the samples may be related to the isolation of Fe^{3+} cations and the interaction of $\text{Fe}^{3+}-\square-\text{Fe}^{3+}$ pairs where the isolated Fe^{3+} cations contributed to the paramagnetism, whereas the $[\text{Fe}^{3+}-\square-\text{Fe}^{3+}]$ versus $[\text{Fe}^{3+}-\square-\text{Fe}^{3+}]$ interaction was favored for antiferromagnetism. However, unlike single Fe cation dopants, the complex incorporation of Sm cations at the A-site in the perovskite structure displayed a new way of enhancing the performance properties of the samples. The Na^+ vacancies were possibly created due to the incorporation of Sm^{3+} at the Na^+ site. The Na^+ vacancies exhibited ferromagnetism [13]. In fact, the origin of the ferromagnetism in Sm- and Fe-co-doped $\text{Bi}_{0.5}\text{Na}_{0.5}\text{TiO}_3$ materials needs further investigation through first principle calculation. However, the ferromagnetism with a greatly enhanced magnetic moment must be applied to electronic devices.

Figure 5 shows the photoluminescence (PL) spectra of the BNSTFO materials through a blue light with a wavelength 475 nm at room temperature. Under the resonant excitation at 475 nm, the four main broad bands with peaks around 567, 601, 647, and 712 nm were obtained from the intra $f-f$ transition of Sm^{3+} cations. Our results are consistent with those of recent reports on the photoluminescence of Sm-doped $\text{Bi}_{0.5}\text{Na}_{0.5}\text{TiO}_3$ materials [23]. The broad main PL spectra present the characteristics of transition from $^4\text{G}_{5/2}$ to $^6\text{H}_{5/2}$, $^6\text{H}_{7/2}$, $^6\text{H}_{9/2}$, and $^6\text{H}_{11/2}$. The highest intensity was obtained

for the transition from ${}^4G_{5/2}$ to ${}^6H_{7/2}$ at the wavelength of approximately 601 nm, which corresponded to the reddish-orange emission [23]. The strong PL of $\text{Bi}_{0.5}\text{Na}_{0.5}\text{TiO}_3$ via the co-doping of Fe and Sm observed at room temperature was addressed by the pure $\text{Bi}_{0.5}\text{Na}_{0.5}\text{TiO}_3$ materials.

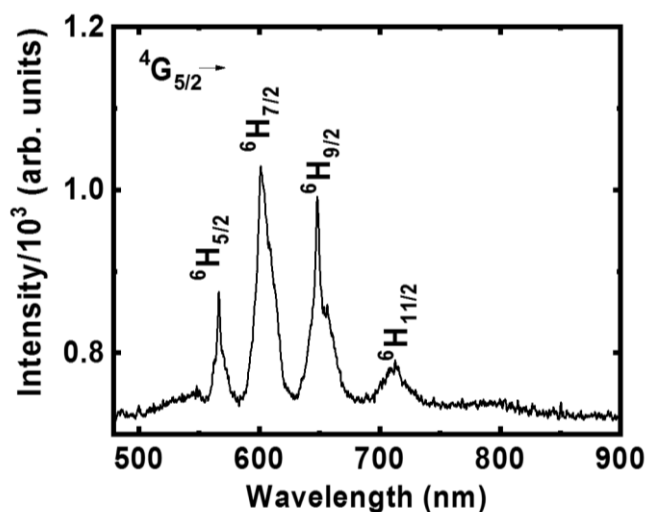


Figure 5. The photoluminescence of BSNTFO samples at room temperature

3. Conclusions

Strong photoluminescence and ferromagnetism were integrated for the first time in lead-free ferroelectric $\text{Bi}_{0.5}\text{Na}_{0.5}\text{TiO}_3$ materials via co-dopants Sm and Fe. A strong room temperature ferromagnetism was obtained with a great magnetization enhancement of up to approximately 19.5 emu/g. The weakly photoluminescent properties of ferroelectric materials were addressed through inner $f-f$ transition. We expect our work to provide a new direction for developing lead-free ferroelectric materials for smart electronic device applications.

Acknowledgement: This research is funded by the Vietnam National Foundation for Science and Technology Development (NAFOSTED) under Grant number 103.02-2015.89.

REFERENCES

- [1] B. Jaffe, W.R. Cook, and H. Jaffe, 1971. *Piezoelectric Ceramics*, Academic, London.
- [2] W. Jo, R. Dittmer, M. Acosta, J. Zang, C. Groh, E. Sapper, K. Wang, and J. Rodel, 2012. *Giant electric-field-induced strains in lead-free ceramics for actuator applications- status and perspective*. *J. Electroceram.* **29**, 71-93.
- [3] S. Tong, Y. E. von Schirnding, and T. Prapamontol, 2000. *Environmental lead exposure: a public health problem of global dimensions*. *Bull. World Health Organ.* **78**, 1068-1077.

- [4] N. D. Quan, L. H. Bac, D. V. Thiet, V. N. Hung, and D. D. Dung, 2014. *Current development in lead-free $Bi_{0.5}(Na,K)_{0.5}TiO_3$ -based piezoelectric materials*. Adv. Mater. Sci. Eng. **2014**, 365391.
- [5] G. A. Smolensky, V. A. Isupov, A. I. Agranovskaya, and N. N. Krainic, 1960. *Dielectric polarization of a series of compounds of complex composition*. Fiz. Tverd. Tela **2**, 2982-2985.
- [6] M. Naderer, T. Kainz, D. Schutz, and K. Reichmann, 2014. *The influence of Tinnonstoichiometry in $Bi_{0.5}Na_{0.5}TiO_3$* . J. European Ceram. Soc. **34**, 663-667.
- [7] Y. S. Sung, J. M. Kim, J. H. Cho, T. K. Song, M. H. Kim, H. H. Chong, T. G. Park, D. Do, and S. S. Kim, 2010. *Effects of Na nonstoichiometry in $(Bi_{0.5}Na_{0.5+x})TiO_3$ ceramics*. Appl. Phys. Lett. **96**, 022901.
- [8] Y. S. Sung, J. M. Kim, J. H. Cho, T. K. Song, M. H. Kim, and T. G. Park, 2011. *Effects of Bi nonstoichiometry in $(Bi_{0.5+x}Na_{0.5})TiO_3$ ceramics*. Appl. Phys. Lett. **98** 012902.
- [9] L. T. H. Thanh, N. H. Tuan, L. H. Bac, D. D. Dung, and P. Q. Bao, 2016. *Influence of fabrication condition on the microstructural and optical properties of lead-free ferroelectric $Bi_{0.5}Na_{0.5}TiO_3$ materials*. Commun. Phys. **26**, 51-57.
- [10] D. D. Dung, N. T. Hung, and D. Odkhuu, 2019. *Magnetic and optical properties of $MgMnO_{3-\delta}$ -modified $Bi_{0.5}Na_{0.5}TiO_3$ materials*. J. Magn. Magn. Mater. **482**, 31-37.
- [11] L. T. H. Thanh, N. B. Doan, N. Q. Dung, L. V. Cuong, L. H. Bac, N. A. Duc, P. Q. Bao, and D. D. Dung, 2017. *Origin of room temperature ferromagnetism in Cr-doped lead-free ferroelectric $Bi_{0.5}Na_{0.5}TiO_3$ materials*. J. Electron. Mater. **46**, 3367-3372.
- [12] L. T. H. Thanh, N. B. Doan, L. H. Bac, D. V. Thiet, S. Cho, P. Q. Bao, and D. D. Dung, 2017. *Making room-temperature ferromagnetism in lead-free ferroelectric $Bi_{0.5}Na_{0.5}TiO_3$ materials*. Mater. Lett. **186**, 239-242.
- [13] L. Ju, C. Shi, L. Sun, Y. Zhang, H. Qin, and J. Hu, 2014. *Room-temperature magnetoelectric coupling in nanocrystalline $Na_{0.5}Bi_{0.5}TiO_3$* . J. Appl. Phys. **116**, 083909.
- [14] Y. Zhang, J. Hu, F. Gao, H. Liu, and H. Qin, 2011. *Ab initio calculation for vacancy-induced magnetism in ferroelectric $Na_{0.5}Bi_{0.5}TiO_3$* . Comput. Theor. Chem. **967**, 284-288.
- [15] Y. Wang, G. Xu, X. Ji, Z. Ren, W. Weng, P. Du, G. Shen, and G. Han, 2009. *Room-temperature ferromagnetism of Co-doped $Na_{0.5}Bi_{0.5}TiO_3$: diluted magnetic ferroelectrics*. J. Alloys Compound. **475**, L25-L30.
- [16] D. D. Dung, N. B. Doan, N. Q. Dung, N. H. Linh, L. H. Bac, L. T. H. Thanh, N. N. Trung, N. V. Duc, L. V. Cuong, D. V. Thiet, and S. Cho, 2019. *Tunable magnetism of $Na_{0.5}Bi_{0.5}TiO_3$ materials via Fe defects*. J. Supercond. Nov. Magn. **32**, 3011-3018.
- [17] N. T. Hung, L. H. Bac, N. T. Hoang, P. V. Vinh, N. N. Trung, and D. D. Dung, 2018. *Structural, optical, and magnetic properties of $SrFeO_{3-\delta}$ -modified $Bi_{0.5}Na_{0.5}TiO_3$ materials*. Physica B **531**, 75-78.
- [18] N. T. Hung, L. H. Bac, N. N. Trung, N. T. Hoang, P. V. Vinh, and D. D. Dung, 2018. *Room-temperature ferromagnetism in Fe-based perovskite solid solution in lead-free ferroelectric $Bi_{0.5}Na_{0.5}TiO_3$ materials*. J. Magn. Magn. Mater. **451**, 183-186.

- [19] M. Zannen, A. Lahmar, M. Dietze, H. Khemakhem, A. Kaadou, and M. E. Souni, 2012. *Structural, optical, and electrical properties of Nd-doped $\text{Na}_{0.5}\text{Bi}_{0.5}\text{TiO}_3$* . Mater. Chem. Phys. **134**, 829-833.
- [20] M. Zannen, M. Dietze, H. Khemakhem, A. Kabadou, and M. E. Souni, 2014. *The erbium's amphoteric behavior effects on sodium bismuth titanate properties*. Ceram. Inter. **40**, 13461-13469.
- [21] R. K. Prusty, P. Kuruva, U. Ramamurty, and T. Thomas, 2013. *Correlations between mechanical and photoluminescence properties in Eu doped sodium bismuth titanate*. Solid State Commun. **173**, 38-41.
- [22] T. Wei, F. C. Sun, C. Z. Zhao, C. P. Li, M. Yang, and Y. Q. Wang, 2013. *Photoluminescence properties in Sm doped $\text{Bi}_{1/2}\text{Na}_{1/2}\text{TiO}_3$ ferroelectric ceramics*. Ceram. Inter. **39**, 9823-9828.
- [23] H. Sun, D. Peng, X. Wang, M. Tang, Q. Zhang, and X. Yao, 2011. *Strong red emission in Pr doped ($\text{Bi}_{0.5}\text{Na}_{0.5}$) TiO_3 ferroelectric ceramics*. J. Appl. Phys. **110**, 016102.
- [24] R. D. Shannon, 1976. *Revised effective ionic radii and systematic studies of interatomic distances in halides and chalcogenides*. Acta. Cryst. A **32**, 751.
- [25] M. K. Niranjan, T. Karthik, S. Asthana, J. Pan, and U. V. Waghmare, 2013. *Theoretical and experimental investigation of Raman modes, ferroelectric and dielectric properties of relaxor $\text{Na}_{1/2}\text{Bi}_{1/2}\text{TiO}_3$* . J. Appl. Phys. **113**, 194106.
- [26] J. Zhu, J. Zhang, K. Jiang, H. Zhang, Z. Hu, H. Luo, and J. Chu, 2016. *Coexistence of ferroelectric phases and phonon dynamics in relaxor ferroelectric $\text{Na}_{0.5}\text{Bi}_{0.5}\text{TiO}_3$ based single crystals*. J. American Ceram. Soc. **99**, 2408-2414.
- [27] M. D. Jr. Domenico, S. H. Wemple, S. P. S. Porto, and P. R. Buman, 1968. *Raman spectrum of single-domain BaTiO_3* . Phys. Rev. **174**, 522-530.
- [28] J. C. Sczancoski, L. S. Cavalcante, T. Badapanda, S. K. Rout, S. Panigrahi, V. R. Mastelaro, J. A. Varela, M. S. Li, and E. Longo, 2010. *Structure and Optical Properties of $[\text{Ba}_{1-x}\text{Y}_{2x/3}](\text{Zr}_{0.25}\text{Ti}_{0.75})\text{O}_3$ Powders*. Solid State Sci. **12**, 1160-1167.
- [29] B. K. Barick, K. K. Mishra, A. K. Arora, R. N. P. Choudhary, and D. K. Pradhan, 2011. *Impedance and Raman spectroscopic studies of ($\text{Na}_{0.5}\text{Bi}_{0.5}$) TiO_3* . J. Phys. D: Appl. Phys. **44**, 355402.
- [30] Baedi, F. Mircholi, and H. G. Moghadam, 2015. *Study of electronic and optical properties of $\text{Bi}_{0.5}\text{Na}_{0.5}\text{TiO}_3$, BiTiO_3 , NaTiO_3 crystals using full potential linear argumented plane wave method*. Optik **126**, 1505-1509.